European Journal of Radiology 118 (2019) 245–250

Contents lists available at ScienceDirect

European Journal of Radiology

journal homepage: www.elsevier.com/locate/ejrad

Research article

Exploratory study of the interest of MR susceptibility-weighted imaging for the pre-operative assessment of pelvic endometriosis extent

Louis Pin[a,*], Anne-Coline Monseau-Thiburce[b], Caroline Ziade-Coularis[a], Alice Benjamin[a], Fanny Menut[a], Jean-Luc Brun[c], Benjamin Merlot[b], Jean-François Chateil[a,d]

[a] Service d'imagerie anténatale, de l'enfant et de la femme, Hôpital Pellegrin, CHU de Bordeaux, Place Amélie Raba- Léon, 33076 Bordeaux Cedex, France
[b] Service d'imagerie médicale, Clinique Tivoli Ducos, 220 rue Mandron, 33000 Bordeaux Cedex, France
[c] Service de chirurgie gynécologique, Maternité Centre Aliénor d'Aquitaine, Place Amélie Raba-Léon, 33076 Bordeaux Cedex, France
[d] CRMSB, UMR 5536, CNRS/University of Bordeaux, 146 rue Léo Saignat, 33076 Bordeaux Cedex, France

ARTICLE INFO

Keywords:
Endometriosis
MRI
Susceptibility-weighted imaging

ABSTRACT

Objective: To evaluate the performance of magnetic resonance imaging (MRI) with susceptibility-weighted imaging (SWI) in the assessment of endometriosis.

Material and methods: This prospective study was performed during the diagnostic step or the pre-operative assessment of endometriosis, between June 2017 and April 2018. The MRI was conducted with a 3T MRI device; protocol included T2W, T1W, with and without fat-saturation sequences completed with a SWI sequence: T2-star weighted angiography (SWAN). The diagnostic performance values of MRI and inter-observer agreement were first evaluated with a conventional MR protocol and then with the complementary SWAN sequence by 2 readers. MRI results were correlated with surgical findings in patients who underwent laparoscopy.

Results: 74 patients were included in the study, and among them 10 patients were treated by laparoscopy. 81% of the endometriosis lesions had signal losses on the SWAN sequence related to hemorrhagic character whereas only 52% of the lesions had T1-weighted hyperintense implants. Diagnostic performance of the MRI examination was improved by the use of the SWAN sequence compared to the conventional MR protocol (Se = 94% and Spe = 73% in complete protocol and Se = 88% and Spe = 69% in conventional protocol), especially for the involvement of torus uterinus, utero-sacral ligament and retro-cervical site. An excellent interobserver agreement (κ-value = 0,94) was noted between the two readers.

Conclusion: SWI can improve the diagnostic accuracy of MRI by allowing the detection of hemorrhagic character of endometriosis lesions.

1. Introduction

Endometriosis is one of the most common gynecological diseases in women of childbearing age, affecting 10% of them. It is defined as a common benign and chronic gynecologic disorder which is related to the ectopic presence of endometrial glands and stroma outside the uterine cavity and responds to the ovarian hormones in the same way as the endometrium during the menstrual cycle [1]. Endometriosis has been shown to cause adhesions, local inflammatory reaction and symptoms such as chronic pelvic pain, dysmenorrhea, dyspareunia and/or a variable level of infertility. However, there is no correlation between severity of symptoms and extent of the disease.

Endometriosis is divided into three forms:

- ovarian endometrioma;
- superficial endometriosis corresponding to hemorrhagic foci on the surface of the peritoneum;
- deep infiltrating endometriosis that is defined as a sub-peritoneal infiltration.

The most common endometriosis sites are the ovaries, torus uterinus, uterosacral ligaments, posterior vaginal fornix, rectum and urinary tract [2].

The treatment of deep infiltrating endometriosis might be medical

Abbreviations: MRI, magnetic resonance imaging; SWAN, star-weighted angiography; SWI, susceptibility-weighted imaging; TR, repetition time; TE, echo time; USL, utero-sacral ligament

* Corresponding author.
E-mail addresses: louispin@hotmail.fr (L. Pin), caroline.ziade@chu-bordeaux.fr (C. Ziade-Coularis), jean-luc.brun@chu-bordeaux.fr (J.-L. Brun), jean-françcois.chateil@chu-bordeaux.fr (J.-F. Chateil).

https://doi.org/10.1016/j.ejrad.2019.06.018
Received 17 September 2018; Received in revised form 20 February 2019; Accepted 23 June 2019

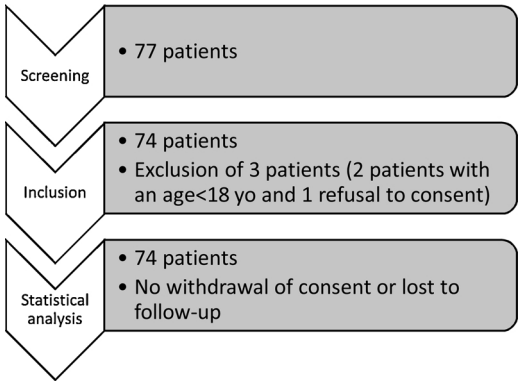

Fig. 1. Flow-chart of the study.

Table 1
Baseline characteristics of study population.

	Average	Median	Min	Max
Age (years old)	33,04	33	18	51
Menarche (years)	12,92	13	10	16
Gravidity (patients)	G0	G1	G2	G3 or more
	39	18	8	9
Parity (patients)	P0	P1	P2	P3 or more
	51	16	3	4

or surgical depending on the stage of the disease and the clinical symptoms. If the patient should undergo surgery, the preoperative imaging assessment should be able to guide the surgeon to perform the most appropriate surgical one-step procedure [3]. Indeed, laparoscopy has limitations in detecting endometriosis lesions hidden by adhesions and knowledge of the precise location of endometriosis is essential for a successful surgical treatment.

Ultrasonography is the first-line imaging modality for the assessment of pelvic endometriosis but has limitations with respect to field-of-view and operator-dependence [4].

Magnetic resonance imaging (MRI) is considered as the best non-invasive imaging method to confirm the diagnosis of deep infiltrating endometriosis and establish a precise mapping of the lesions before surgery [5]. The diagnosis of endometriotic locations is usually facilitated by the detection of their hemorrhagic features on fat suppression T1-weighted images. However, diagnosis can be challenging because some lesions contain only punctate foci of high-signal intensity on T1 sequences representing minimal cyclical bleeding, surrounded by fibrosis and smooth muscle hypertrophy. Also, detection of the superficial form of endometriosis is limited with current imaging techniques and small non-hemorrhagic foci are often not detectable.

Susceptibility-weighted imaging (SWI) is a 3D, flow-compensated, radiofrequency spoiled gradient-recalled echo sequence that takes advantage of susceptibility variations between tissues and yields high sensitivity for blood by-products detection [6]. The magnetic susceptibility effects generated by local inhomogeneity of the magnetic field are visualized as a signal void. Unlike T1-weighted sequences, SWI can detect not only subacute blood by-products like methemoglobin, but also chronic blood by-products such as hemosiderin. Since endometriosis lesions are chronic cyclical hemorrhagic lesions, and therefore rich in blood by-products, SWI-MRI could be useful in the preoperative assessment of endometriosis, and eventually in superficial peritoneal lesion detection. Mainly used in neuroimaging studies, SWI have recently been applied to pelvic imaging [7] but only a few studies have reported their findings in the evaluation of endometriosis [8].

The purpose of our study is to evaluate the performance of MRI with SWI in the assessment of endometriosis.

Table 2
Clinical parameters of study population.

Symptoms	Pelvic pain 72%	Dyspareunia 24%	Dysmenorrhea 33%	Fertility disorders 13%	
Medical treatment	Absent 55%	Estroprogestative pills 18%	Progestogens 12%	GnRH Agonists 5%	Others 10%
Previous surgical treatment	Absent 39%	Curative laparoscopy 32%	Exploratory laparoscopy 12%	Appendicectomy 9,5%	Others 7,5%
Period of Menstrual cycle at time of MRI	Undetermined 26%	Menstrual period (D1–D5) 15%	Follicular phase (D6–D12) 25,7%	Ovulatory phase (D13–D15) 20,3%	Luteal phase (D16–D28) 13,5%

Table 3
Correlation between MR Imaging Results and Surgical Findings.

Endometriosis locations	Conventional MRI protocol				Complete MRI protocol (reader 1)				Complete MRI protocol (reader 2)			
	Se (%)	Spe (%)	PPV (%)	NPV (%)	Se (%)	Spe (%)	PPV (%)	NPV (%)	Se (%)	Spe (%)	PPV (%)	NPV (%)
Pelvic endometriosis	88,2	68,8	68,2	88,5	94,1	73,3	72,7	94,3	94,1	71,1	71,1	94,1
Endometriomas	100	60	50	100	100	60	50	100	100	60	50	100
Torus/USL	93,7	64,3	75	90	93,7	71,4	78,9	90,9	93,7	71,4	78,9	90,9
Retro-cervical site	50	83,3	66,6	71,4	100	100	100	100	100	83,3	66,6	100
Intestinal involvement	83,3	100	100	83,3	83,3	100	100	83,3	83,3	100	100	83,3

Se: sensibility, Spe: specificity, PPV: positive predictive value, NPV: negative predictive value.

Table 4
Site mapping of MRI-signal endometriosis lesions with laparoscopic correlation (operated patients).

Endometriosis sites	High-intensity on T1W	Signal void on SWI	Surgical findings
Endometriomas	8	8	8
Torus uterinus	2	4	5
Utero-sacral ligaments	4	10	11
Retrocervical area	2	4	4
Intestinal involvement	3	5	6
Abdominal wall	1	1	1
Douglas pouch	1	1	3
Fallopian tubes	0	0	2
Broad ligament	0	0	1
External adenomyosis	1	1	1

T1W: T1-weighted imaging, SWI: susceptibility-weighted imaging.

Table 5
Site mapping of MRI-signal comparisons of endometriosis lesions (non-operated patients).

Endometriosis sites	MRI findings on T2W	High-intensity on T1W	Signal void on SWI
Endometrioma	25	25	23
Fallopian tube	5	4	5
Torus uterinus	20	10	15
Utero-sacral ligament	67	16	63
Retrocervical area	8	6	7
Intestinal involvement	15	6	11
External adenomyosis	2	2	2
Abdominal wall	3	2	3
Vesico-uterine pouch	2	0	1
Round ligament	7	2	6
Broad ligament	3	1	1
Pelvic wall	2	2	1
Surgical scar	2	2	2

T2W: T2-weighted imaging, T1W: T1-weighted imaging, SWI: susceptibility-weighted imaging.

2. Material & methods

2.1. Study population

The study was approved by the local ethics committee and informed written consent was obtained from all individual participants included in the study (ID-RCB: 2017-A00698-45).

This prospective, comparative and monocentric study consecutively included patients who underwent MRI in our institution between June 2017 and April 2018. Inclusion criteria in this study were: to be a woman over 18 years-old, to be referred to the women's imaging department for diagnostic or pre-operative work-up of endometriosis, affiliated or beneficiary of a social security system and providing signed written consent for the study. The criteria for non-inclusion were: to be younger than 18 years old, to be pregnant or breastfeeding, to be defended by legal protection or having a contraindication to MRI. An examination was performed before the MRI was conducted and patients were duly informed.

2.2. MRI technique

MR imaging was performed using a 3 T MR imaging device (Discovery 750 W, General Electric [Milwaukee, WI]) with a dedicated pelvic phased array coil (32 channels). Imaging was performed regardless of the stage of the menstrual cycle. All the patients received an intramuscular antispasmodic drug (Scoburen® 20 mg/ml) 10 min before imaging to decrease bowel peristaltic movements. A self-administered cleansing enema 12 h and 2 h before the start of the examination was also required. A systematic vaginal or rectal opacification (ultrasound gel) was not mandatory.

The conventional protocol always included free breathing acquisitions consisting of sagittal fast spin echo T2-weighted sequences (TR/TE 10486/95 ms, flip angle 120°, slice thickness 4 mm, field of view 240 x 240 mm), axial fast spin echo T2-weighted images obtained from the renal hilum to pelvic floor (TR/TE 9549/61 ms, flip angle 142°,slice thickness 5 mm, field of view 320 × 320 mm), a 3D T2-weighted sequence (TR/TE :1800/114 ms, field of view 340 × 340 mm, slice thickness 1 mm) and LAVA-flex sequence who provided T1-weighted imaging with and without fat suppression (TR/TE : 6,2 ms/1,2 ms, flip angle 12°, slice thickness 2,4 mm, field of view 340 × 340 mm).

After completion of the conventional MR protocol, additional SWI sequence was performed (axial 3D SWAN, General Electrics), using magnitude and phase information (TR/TE 50/24,6 ms, flip angle 15°, field of view 240 × 240 mm, matrix 512 × 512, slice thickness 1,4 mm). The duration of SWAN sequence was 4 min.

2.3. MRI analysis

The images were independently analyzed by two radiologists with a various experience in MRI women's imaging. Reader 1 was a junior radiologist who had 5 years of general experience in MR imaging and reader 2 was highly experienced in gynecologic imaging (8 years). Each one was asked to determine the presence or absence of endometriosis using a checklist precising the location, whether it was a superficial or deep form of endometriosis and the MRI signal for each pelvic location that was found. The presence of a hyper-intense signal on fat suppression T1-weighted images and a susceptibility artifact (signal void) on SWAN sequence was considered as hemorrhagic foci. The overall quality of SWAN sequence was rated as good, average or poor.

Radiologists first examined together the "conventional MRI protocol" (i.e., sagittal and axial SE-T2-weighted images, 3D T2-weighted sequence, T1-weighted images with and without fat suppression) for all patients. For patients who underwent surgery, a second reading was performed; each reader had a separate blind examination of "complete MRI protocol" with the addition of SWAN sequence. The time interval between the readings was at least 4 weeks to minimize recall bias. The readers were blinded to surgical findings.

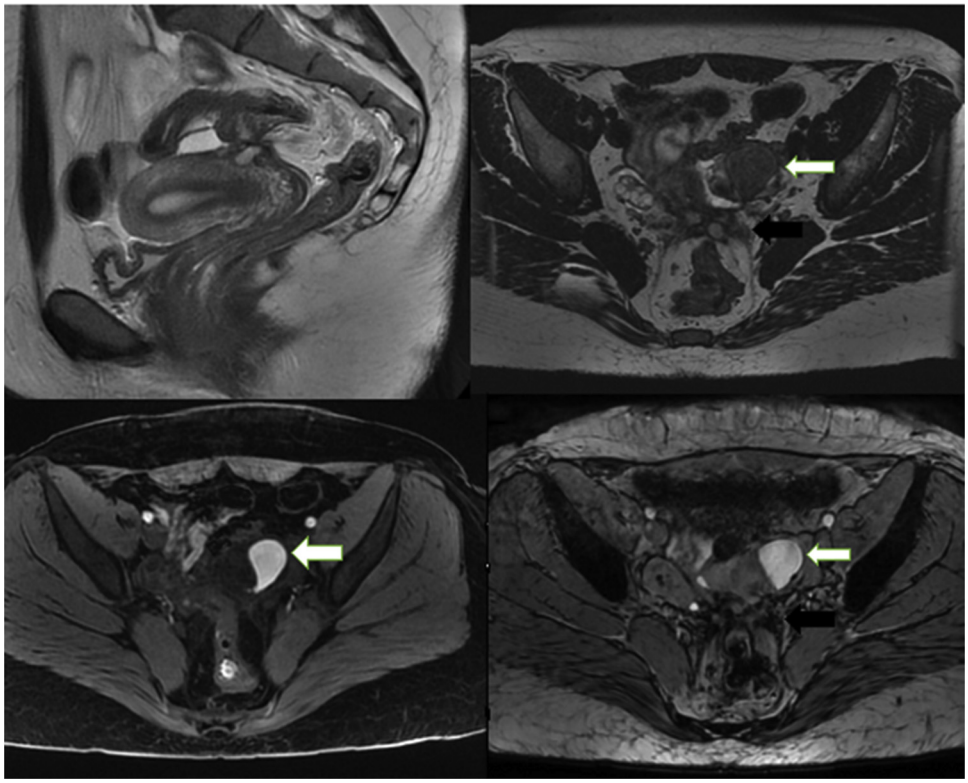

Fig. 2. A 28-year-old woman presented fertility disorder. A) Sagittal T2-weighted sequence demonstrates posterior endometriosis of the uterus. B) Axial T2-weighted sequence shows a left cystic mass (white arrow) presenting shading, an involvement of torus uterinus and a thickening of the two USL (black arrow). C) Axial fat saturated T1-weighted sequence demonstrate hyperintense cyst defining an endometrioma, without hyperintense foci of the two USL. D) Axial SWAN sequence reveals the hemorrhagic character of the USL.

2.4. Surgical findings

Surgical findings were considered as gold standard. All locations of endometriosis were recorded in a surgical location check-list differentiating superficial and deep form of endometriosis. Histopathological analysis was not performed.

2.5. Statistical analysis

Qualitative variables are described as frequencies and percentages.

To evaluate the diagnostic performance, the measures of sensitivity, specificity, positive predictive value and negative predictive value were estimated from the associated contingency table. Diagnostic performance values of MRI were only evaluated for the patients who underwent laparoscopic exploration.

The interobserver agreement between the two readers for the diagnosis of the different endometriosis locations was quantified using the Kappa coefficient; a κ-value of less than 0.40 was considered to represent a poor agreement; 0.40–0.80 a good agreement and greater than 0.80 an excellent agreement.

MRI signal of endometriosis lesions in T1-weighted images and in SWAN sequence were compared using percentages, by analyzing endometriosis lesions found in laparoscopy (for operated patients) and lesions found in conventional T2-weighted images (for non-operated patients).

3. Results

3.1. Study population

Among 77 consecutive patients, the study included 74 patients and all their MRI studies were analyzed (Fig. 1). None had been excluded because of withdrawal of consent, lost to follow-up or poor-quality imaging. No serious adverse events have been reported after the MRI.

Tables 1 and 2 summarize the baseline characteristics and the clinical parameters of study population. Positive diagnosis of endometriosis with imaging was confirmed in 74% of all patients (55/74).

3.2. Surgical results

Ten out of seventy-four patients (13%) were treated with laparoscopy. A total of 42 endometriosis lesions including superficial peritoneal implants (19), endometriomas and deep pelvic endometriosis locations were removed from the 10 patients. Sites of lesions included mainly the torus uterinus (5/10), one or the two uterosacral ligaments (11/20), the recto-sigmoid (6/10), the retrocervical area (4/10) and ovaries (8 endometriomas).

3.3. MRI analysis

Quality of the SWI sequence was rated as optimum, sub-optimum and poor in respectively 30%, 65% and 5% of cases.

Among the ten patients with surgically proved involvement, the diagnostic performances were first evaluated with MRI conventional protocol and then with additional contribution of SWAN sequence at the second examination. The sensitivity, specificity, positive and negative predictive values of MRI for the diagnosis of pelvic endometriosis and for each specific location are summarized in Table 3.

In the end, 34 out of 42 (81%) endometriosis locations were detected by signal-intensity losses on SWI whereas 22 out of 42 endometriosis locations (52%) were detected by their high-signal intensity on T1W. MRI findings with laparoscopic correlation are listed in Table 4.

An excellent interobserver agreement was noted between different readers for all deep endometriotic locations (κ-value = 0,94).

Regarding superficial endometriosis, surgical exploration revealed 19 implants, (8 ovarian fossae involvement, 4 utero-sacral ligaments involvement and 2 pouch of Douglas involvement). Ovarian fossa involvement was effectively recognized using the T1-weighted sequence only, as well as 3/4 USL locations. In total, 12 lesions were effectively detected with conventional protocol, but an additional lesion of the

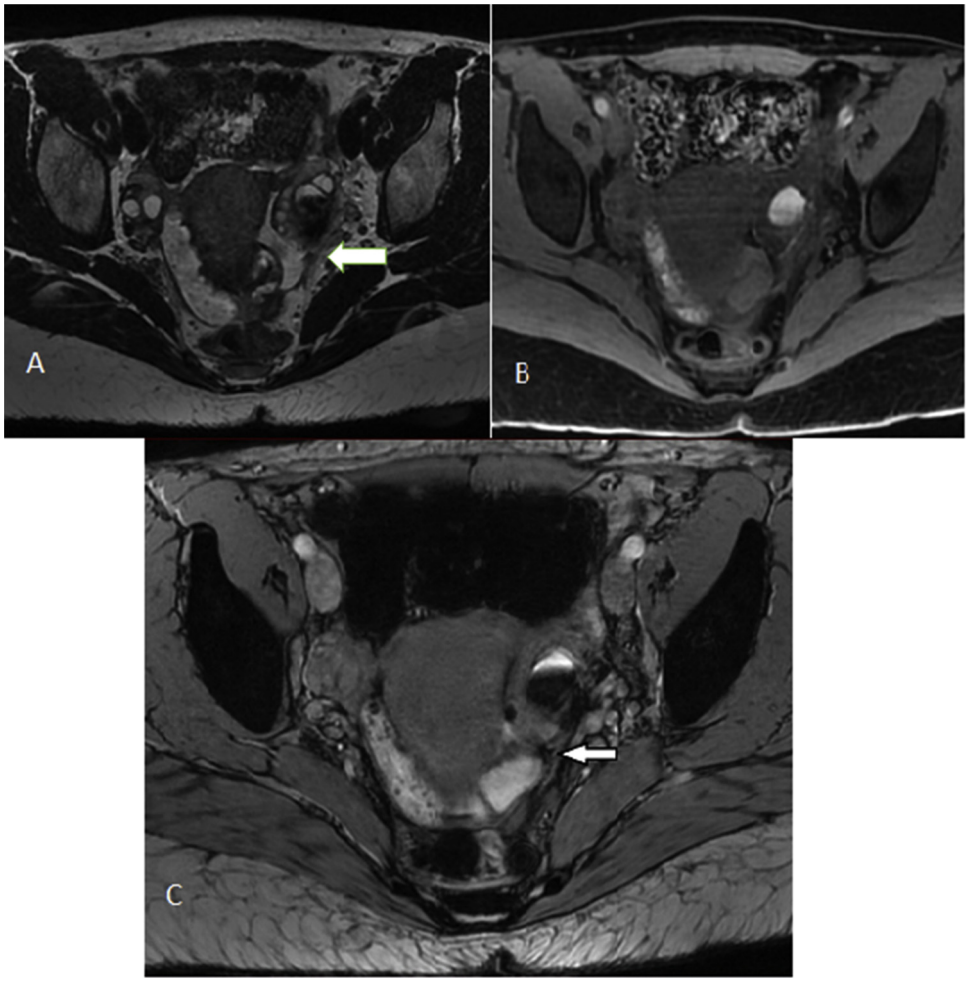

Fig. 3. A 35-year-old woman presented with cyclic pelvic pain. A) Axial T2-weighted sequence shows a left cystic mass presenting shading and a no specific thickening of the left USL (arrow). B) Axial fat saturated T1-weighted sequence shows hyperintense cyst defining an endometrioma. There is no hyperintense foci within the left USL.C) Axial SWAN sequence confirms the presence of the endometrioma and reveals the hemorrhagic character of left USL (arrow).

vesico-uterine pouch was detected with the contribution of the SWAN sequence.

Among the sixty-four patients without surgically proved pelvic endometriosis, T2-weighted imaging revealed a broad spectrum of pelvic endometriosis locations. Signal of endometriosis lesions visualized in T2-weighted imaging was evaluated and compared with T1-weighted imaging and SWAN sequence: MRI findings of these locations are listed in Table 5.

4. Discussion

Pelvic endometriosis typically consists of endometrial stroma and glands, with respect to the hormonal changes during phases of menstrual cycle. Endometriosis has a large spectrum of imaging features, but the hemorrhagic nature of the lesions is an essential element in their characterization [9].

Laparoscopy is the gold standard for evaluation and treatment of endometriosis lesions but a complete preoperative assessment must be performed to guide the surgical treatment. So far, MRI is the best imaging modality for the staging of pelvic endometriosis [10].

SWI is a MR technique which is sensitive to blood-by products including methemoglobin and hemosiderin. It combines information concerning the phase and magnitude from velocity-compensated gradient-echo sequence. The magnetic susceptibility effect generated by local inhomogeneity of the magnetic field caused by hemorrhagic products are visualized as signal void. The SWI sequence is usually used in neuro-imaging to explore tumors, vascular malformation, trauma, stroke and microhemorrhages [11].

In medical literature, only few studies have explored the use of SWI other than neuro-imaging. Solak et al. reported the signal changes of abdominal wall endometriosis during the menstrual cycle [12]. Takeuchi et al. reported that SWI improved the characterization of endometrioma by detecting signal void along the cyst wall as hemosiderin deposition [8]. Takeuchi et al. showed that signal voids as hemorrhagic component on SWI were also observed in extra-ovarian endometriosis [13]. Finally, Cimsit et al. reported that SWI provides additional value to improve diagnostic ability of pelvic MRI in endometriosis [14].

Our study demonstrated that SWAN might be a useful additional sequence for treatment planning of endometriosis. The overall diagnostic performances of MRI with SWI were improved regarding the evaluation of adnexal and deep infiltrating endometriosis with an increase of the sensitivity from 88,2% to 94,1% and specificity from 68,8% to 73,3%.

As reported by Bazot, we found that the torus uterinus and the USL were the anatomic structures most frequently involved with deep pelvic endometriosis [15]. Endometriosis lesions of torus uterinus and USL appeared with signal voids in SWAN sequence with a frequency of 87,5% and 90% of cases, indicating a hemorrhagic character. This data allowed to improve specificity from 64,3% to 71,4% for this particular location of endometriosis (Fig. 2).

Furthermore, SWAN sequence also improves the evaluation of retrocervical area with an increase of the sensitivity from 50% to 100%.

Signal voids were presents on SWAN sequence with a prevalence of 100% and 88% in the operated and non-operated population respectively. However, when SWAN sequence was added to the conventional MR protocol, no significant increase in accuracy was demonstrated for the diagnosis of intestinal endometriosis and endometriomas. Possible limiting factors for rectosigmoid involvement evaluation may be the presence of susceptibility artifacts caused by intestinal gas. Diagnosis of endometriomas with conventional protocol has a reported sensitivity and specificity of 95% and 91% respectively in the medical literature [16]. Such high diagnostic performance values may explain the lack of interest of the SWAN sequence for this particular location.

The hemorrhagic character of endometriosis lesions of any studied location was more frequently demonstrated with SWAN than with conventional T1-weighted sequence (Fig. 3).

Diagnosis of abdominal wall endometriosis can be difficult but our study found that all of these lesions (4/4) had magnetic susceptibility characteristics.

A part of this work was to study superficial form of endometriosis. Our study reported a sensitivity of 63% with conventional MR protocol but only one additional implant was detected with SWAN sequence, probably due to the presence of many artefacts of magnetic susceptibility, more prominent at 3T [17]. Further comparative study may be useful to determine which field strength is suitable for evaluation of superficial form of endometriosis with SWI.

We acknowledge that our study has several limitations. First, a small sample of patients underwent laparoscopic endometriosis surgery. Studies with larger groups are needed to support our findings. Secondly, susceptibility artefacts caused by intestinal gas may mask the detection of signal voids caused by blood-products within small endometriosis foci. Thirdly, the analysis of the anterior and lateral compartments was sub-optimal because of the low prevalence of theses lesions.

5. Conclusion

We conclude that susceptibility-weighted imaging can contribute to the diagnosis of deep infiltrating endometriosis, especially for the characterization of USL and for the detection of retro-cervical area. In contrast, the diagnostic accuracy of MRI was not significantly increased by SWI for the analysis of superficial forms of endometriosis.

Formatting of funding sources

This research did not receive any specific grant from funding agencies in the public, commercial, or not-for-profit sectors.

Declaration of Competing Interest

The authors declared no potential conflicts of interest with respect to the research, authorship and/or publication of this article.

References

[1] P.B. Clement, Pathology of endometriosis, Pathol. Annu. 25 (Pt 1) (1990) 245–295.
[2] C. Chapron, A. Fauconnier, M. Vieira, H. Barakat, B. Dousset, V. Pansini, et al., Anatomical distribution of deeply infiltrating endometriosis: surgical implications and proposition for a classification, Hum. Reprod. 18 (January (1)) (2003) 157–161.
[3] H. Roman, M. Ballester, J. Loriau, M. Canis, P.A. Bolze, J. Niro, et al., Strategies and surgical management of endometriosis: CNGOF-HAS Endometriosis Guidelines, Gynecol. Obstet. Fertil. Senol. 46 (March (3)) (2018) 326–330.
[4] M. Bazot, I. Thomassin, R. Hourani, A. Cortez, E. Darai, Diagnostic accuracy of transvaginal sonography for deep pelvic endometriosis, Ultrasound Obstet. Gynecol. 24 (August (2)) (2004) 180–185.
[5] M. Bazot, E. Darai, R. Hourani, I. Thomassin, A. Cortez, S. Uzan, et al., Deep pelvic endometriosis: MR imaging for diagnosis and prediction of extension of disease, Radiology. 232 (August (2)) (2004) 379–389.
[6] E.M. Haacke, S. Mittal, Z. Wu, J. Neelavalli, Y.-C.N. Cheng, Susceptibility-weighted imaging: technical aspects and clinical applications, part 1, AJNR Am. J. Neuroradiol. 30 (January (1)) (2009) 19–30.
[7] W. Chen, Z. DelProposto, W. Liu, M. Kassir, Z. Wang, J. Zhao, et al., Susceptibility-weighted imaging for the noncontrast evaluation of hepatocellular carcinoma: a prospective study with histopathologic correlation, PLoS One 9 (5) (2014) e98303.
[8] M. Takeuchi, K. Matsuzaki, H. Nishitani, Susceptibility-weighted MRI of endometrioma: preliminary results, AJR Am. J. Roentgenol. 191 (November (5)) (2008) 1366–1370.
[9] E.S. Siegelman, E.R. Oliver, MR imaging of endometriosis: ten imaging pearls, Radiographics 32 (October (6)) (2012) 1675–1691.
[10] I. Thomassin-Naggara, S. Bendifallah, P. Rousset, M. Bazot, M. Ballester, E. Darai, Diagnostic performance of MR imaging, coloscan and MRI/CT enterography for the diagnosis of pelvic endometriosis: CNGOF-HAS Endometriosis Guidelines, Gynecol. Obstet. Fertil. Senol. 46 (March (3)) (2018) 177–184.
[11] S. Mittal, Z. Wu, J. Neelavalli, E.M. Haacke, Susceptibility-weighted imaging: technical aspects and clinical applications, part 2, AJNR Am. J. Neuroradiol. 30 (February (2)) (2009) 232–252.
[12] A. Solak, N. Sahin, B. Genç, A.R. Sever, M. Genç, O.N. Sivrikoz, Diagnostic value of susceptibility-weighted imaging of abdominal wall endometriomas during the cyclic menstrual changes: a preliminary study, Eur. J. Radiol. 82 (September (9)) (2013) e411–416.
[13] M. Takeuchi, K. Matsuzaki, M. Harada, Susceptibility-weighted MRI of extra-ovarian endometriosis: preliminary results, Abdom. Imaging 40 (October (7)) (2015) 2512–2516.
[14] C. Cimsit, T. Yoldemir, M. Guclu, I.N. Akpinar, Susceptibility-weighted magnetic resonance imaging for the evaluation of deep infiltrating endometriosis: preliminary results, Acta radiol. 57 (July (7)) (2016) 878–885.
[15] M. Bazot, C. Lafont, R. Rouzier, G. Roseau, I. Thomassin-Naggara, E. Daraï, Diagnostic accuracy of physical examination, transvaginal sonography, rectal endoscopic sonography, and magnetic resonance imaging to diagnose deep infiltrating endometriosis, Fertil. Steril. 92 (December (6)) (2009) 1825–1833.
[16] V. Nisenblat, P.M.M. Bossuyt, C. Farquhar, N. Johnson, M.L. Hull, Imaging modalities for the non-invasive diagnosis of endometriosis, Cochrane Database Syst. Rev. 2 (February (26)) (2016) CD009591.
[17] J.R. Nair, W. Van Hecke, F. De Belder, C. Venstermans, L. van den Hauwe, J. Van Goethem, et al., High-resolution susceptibility-weighted imaging at 3 T with a 32-channel head coil: technique and clinical applications, AJR Am. J. Roentgenol. 195 (October (4)) (2010) 1007–1014.